JMEPEG (2012) 21:849–853
DOI: 10.1007/s11665-011-9949-5

1059-9495/$19.00

Cavitation Erosion Behavior of HPDL-Treated TWAS-Coated Ti6Al4V Alloy and Its Similarity with Water Droplet Erosion

B.S. Mann, Vivek Arya, and B.K. Pant

(Submitted September 14, 2010; in revised form April 13, 2011)

Twin wire arc-sprayed (TWAS) coating of commercially available SHS 7170-cored wire was obtained on Ti6AL4V alloy, and to improve its properties, it was further surface treated with high-power diode laser (HPDL). The cavitation erosion (CE) resistance of TWAS-coated samples was evaluated as per ASTM G-32-2003 and it was compared with laser-treated and untreated Ti6Al4V alloys. The CE resistance of TWAS-coated SHS 7170 samples after HPDL treatment has improved significantly. The main reasons for its improvement are elimination of pores, increased fracture toughness, reduced hardness, and brittleness. The CE resistance of HPDL-treated TWAS coating is compared with water droplet erosion resistance. It is observed that there is a similarity in the both the phenomenon.

Keywords cavitation and water droplet erosion, diode laser, Ti6Al4V alloy, twin wire arc spraying

1. Introduction

Material damages occurring due to cavitation erosion (CE) are very common in the industry especially in pumps, ship impellers, hydraulic machinery, and high-speed mixers in pharmaceutical industry. The CE phenomenon is understood as the formation of bubbles due to drop in local pressure either due to flow fluctuation (vibration) or due to sudden change in flow. These bubbles travel in a zone of high pressure where they collapse, leading to generation of high-pressure shock waves and jetting of micro jets. Owing to repetitive high-pressure shock waves and jetting action of micro jets, the solid surfaces erode quickly. This becomes one of the main causes of failure of engineering components (Ref 1). On the other hand, water droplet erosion (WDE) damages occurring on the engineering components are due to high impacts of water droplets. When a spherical liquid droplet impacts on a flat solid boundary, a compression wave front is generated, and contact periphery expansion takes place quicker than the compression wave front movement. The compression wave front travels at acoustic speed in the medium, whereas the contact periphery travels much faster than the compression wave front. At a later stage, the compression wave envelop overtakes the contact periphery and jetting action of micro-jets in a manner similar to the jetting action of micro jets in cavitation, causing erosion of material (Ref 2-5). During impact of a liquid column on a solid boundary, the impact pressure generated at the liquid-solid interface is sufficiently high to cause the erosion of materials. The impact pressure on a solid boundary reaches its maximum value of $\sim 3\rho CV$, i.e., three times the water hammer pressure (ρ: liquid density, C: acoustic speed in liquid, and V: droplet impact velocity), and water-jetting velocities become 10-12 times higher than the water droplet impact velocities (Ref 3-5).

Ti6Al4V alloy is widely used in many areas, such as aerospace, military, chemical, and biomedical industries, because of its excellent properties, such as corrosion resistance and high strength-to-weight ratio. To improve WDE and CE resistance of titanium alloys, a number of surface-treatment and coating processes have been adopted and published in Ref 6-9. Information on CE resistance of other materials including TiN nanocrystalline coatings on stainless steel is also available in Ref 10-29. It was concluded in Ref 28 and 29 that the CE resistance of the TiN coatings is related to adhesion, inner defects, and plastic deformation of the coatings which have a correlation with the coating thickness. Among these, laser gas nitriding of titanium alloys appears to be simple and attractive. However, it has the limitation of heating the base material above its melting temperature (>1650 °C), leading to distortions and warpage of the components and maximum depth of increased hardness is limited to a few micron only. Heating of Ti6Al4V alloy components above its melting temperature generally leads to excessive tensile residual stresses which may not be acceptable to the finished components. On the other hand, TiN coatings deposited by PVD provide significantly enhanced surface performance; however, the coating thickness is limited to a few microns, which limits the coating life. Significant study on WDE of Ti6Al4V alloy has been done and is reported in Ref 7-9. It has also been reported that the TWAS SHS $7170^{Plus\ B}$ coating after high-power diode laser (HPDL) treatment has improved the WDE resistance manifold (Ref 8). A good correlation between WDE and CE in case of pure aluminum, alloy steels, and stainless steel has been obtained as details are given in Ref 27. The CE testing was performed by

B.S. Mann, Vivek Arya, and **B.K. Pant**, Surface Coatings and Treatment Laboratory, BHEL, Corporate R&D Division, Vikasnagar, Hyderabad 500093, India. Contact e-mail: mann_balbir@yahoo.com.

cavitating jet as per ASTM G134-95 (2006), and the same jet has been used for water impingement erosion testing. WDE and CE damage mechanisms of different materials, coatings, and surface treatment are available independently in the literature. However, their combined damage mechanism and their correlation are lacking.

In this article, the WDE and CE behaviors of HPDL-treated TWAS SHS $7170^{Plus\ B}$-coated Ti6Al4V alloy have been studied. The coating has been analyzed with scanning electron microscope, and its damage mechanism is discussed in detail. Characterizing of materials and coatings in WDE using rotating wheel as per ASTM G-73-1998 is a cumbersome, expensive, and time-consuming process, whereas evaluating these in CE as per ASTM G-32-2003 or ASTM G-134-95 (2006) is simple, quick, and does not require elaborate arrangements. In the present investigation, these standards are discussed, and the experimental results are analyzed. The revised versions of these standards, as on date, are available as ASTM G-73-2010 and ASTM G-32-2009.

2. Experimental

2.1 Twin Wire Arc Spraying

Using Hobart Tafa 9000 twin wire arc-spraying (TWAS) system, the SHS 7170-cored wire (1.6-mm diameter) was sprayed on ∅ 12.70 mm × 40 mm cylindrical and 30 mm × 30 mm × 100 mm flat Ti6Al4V alloy samples. While TWAS was performed on the samples, the TWAS gun was mounted on six plus two axis robot, and spraying parameters, such as arc voltage, current, spray distance, and rotation and transverse speeds were optimized and controlled. The test samples were grit blasted using 24-mesh alumina grit at an air pressure of 5-5.5 kg/cm^2 (g). The spraying and experimental parameters such as laser surface treatment used in the present investigation were as per Ref 8. A thin boride layer of thickness 70-100 μm is provided in between titanium alloy and TWAS SHS 7170 coating, which has overcome the thermal mismatch and which has resulted in excellent adhesion between the titanium alloy substrate and the TWAS SHS 7170 main coat. The TWAS SHS 7170 coating thickness was maintained in the range of 300-350 μm.

2.2 HPDL Surface Treatment

Standard CE and WDE test samples were machined from Ti6Al4V alloy. These were TWAS coated and later on HPDL heat treated. A fixture was fabricated to hold and to rotate the cylindrical samples while carrying out HPDL surface treatment. For WDE resistance evaluation, cylindrical test samples were used, and for HPDL treatment these were fixed in a self-centered three-jaw chuck one by one at one end and supported by a fixture at the other end. The fixture has a rotating seal, so that the samples can rotate freely, and the air used for cooling the samples does not leak. Rapid cooling of the sample was carried out during HPDL surface treatment by introducing compressed air having the volumetric flow rate of 15-16 m^3/h through the M8-tapped hole inside the samples. This air is capable of removing heat at a rate of 160-180 W which is comparable to the heat removed in a bulk titanium alloy during laser surface treatment. For CE, the flat samples of size 30 × 30 × 100 mm^3 were coated using Hobart Tafa 9000 TWAS system and later on HPDL treated. Standard CE test samples were machined from these flat samples. The samples were thoroughly cleaned using acetone before start of the experiment to make the surface free from dust, oil, etc. Details of HPDL parameters are given in Ref 8.

HPDL surface treatment was carried out on each sample using 4.6-kW Diode Laser System (Laserline GmbH). The laser head was mounted on a six plus two axis robot (Kuka GmbH). Rectangular optics of 20 mm × 2.8 mm was used for the surface treatment of cylindrical samples meeting ASTM G-73-1998 and also for CE test samples meeting ASTM G-32-2003 requirements. Laser beam power was controlled in a closed loop by a two-color pyrometer for achieving uniform surface temperatures. The complete system was controlled by the robot controller. The robot was programmed in such a way that the laser beam tracked the sample at a speed of 1.5-2 mm/s ensuring that hardening of the sample was completed in one pass. After HPDL treatment. All the test samples were stress relieved for 4 h. These samples were then used for WDE and CE testings.

2.3 Droplet Erosion Testing and Other Properties of HPDL-Treated Samples

2.3.1 Droplet Erosion Testing of HPDL-Treated Samples. The details of WDE test facility are given in Ref 7 and 12. In short, the test facility consists of a 700-mm-diameter chamber and a round stainless steel disk where the test samples are positioned. Cylindrical samples, 40 mm in length and 12.70 mm in diameter, are affixed on the periphery of the disk. A precision balance (±0.1 mg) was used for measurement of mass loss before and after testing. The test duration depending upon energy and mass fluxes was selected in such a way as to achieve steady-state erosion in limited number of cycles. The extent of erosion damage is calculated from the mass loss divided by the density of the material. The results have been plotted in the form of cumulative volume loss v/s number of cycles.

2.3.2 Cavitation Erosion Testing. The CE tests as per ASTM G-32-2003 (vibratory ASTM standard) were performed at 20 KHz and 50-μm amplitude at room temperature. Mass loss to an accuracy of 0.01 mg after certain cavitation test duration interval was recorded, and the mean depth of erosion rate (MDER) was calculated. Before evaluating the coating material, commercially pure (99.5%) annealed wrought nickel 200 standard samples were first tested for cavitation. After establishing the accuracy and reliability of the cavitation tester, the coated and uncoated Ti6AL4V test samples were tested. The CE is measured by the MDER which gives the relative performance of the samples and is calculated using the formulas: MDER (μm/h) = 1000 $\Delta V/(A \times \Delta t)$ and Re = 1/MDER (ΔV: volume loss in mm^3, Δt: test duration in hour, A: surface area of the specimen in mm^2, and Re: CE resistance of the specimen in h/μm).

3. Results and Discussions

3.1 Water Droplet and Cavitation Erosion Resistance

It is reported in Ref 8 that by providing a thin boride bond coat and subsequently treating with HPDL, the bonding of TWAS SHS 7170 coating to titanium alloy has improved

manifold. The WDE resistance of this multilayer coating (TWAS SHS 7170$^{Plus\ B}$) has also improved significantly. The WDE test results of laser-treated TWAS SHS 7170$^{Plus\ B}$-coated samples along with laser-treated Ti6Al4V alloy samples are given in Fig. 2. It is seen from the Fig. 2 that the laser-treated TWAS SHS 7170$^{Plus\ B}$-coated sample has performed much better than the laser-treated Ti6Al4V alloy samples. It is also reported that the excellent WDE resistance of TWAS SHS 7170$^{Plus\ B}$ coating after HPDL surface treatment is due to finer grain morphology (Ref 8). The "as-sprayed" TWAS SHS 7170 coating has peeled off during initial WDE testing (~47,500 cycles) because it has inherent voids, pores and inter-boundary defects. The TWAS SHS 7170$^{Plus\ B}$-coated samples were also tested for CE as per ASTM G-32-2003, and the results are given in Fig. 1 and 3. The "as-sprayed" TWAS SHS 7170 coating has also peeled off during initial CE testing (~half an hour). From Fig. 1, 2, and 3, it is seen that the CE and WDE volume loss trends of Ti6Al4V alloy (coated, uncoated, and laser treated) including incubation period are similar. The materials and coatings which have performed excellently well in WDE have also performed very well in CE. There are chances that owing to very high-impact pressure, the water in the form of micro jets may solidify (Ref 30), and WDE and CE may no longer become as liquid impingement wear but instead may become as solid particle wear. The water impact velocity in our test rig is of the order of 147.6 m/s. Assuming an acoustic wave speed of the order of 1500 m/s, the impact pressure of ~663.75 MPa is exerted on the surface (calculated from 3ρCV). The solidification of water, arising due to cavitation bubble collapse generating very high pressure (≥ 1000 MPa) for less than a nano second, has already been experienced and reported in Ref 30. This could be one of the reasons for grain-by-grain material removal.

The water droplet impact velocities occurring in bypass/control valves and low-pressure steam turbine blades are supersonic (approximately 4-5 times that of 147.6 m/s) (Ref 7). Under such situations, the impact pressure generated due to 3ρCV will exceed 2500 MPa. The shock wave speed, jetting time, and pressure generated due to impact of water droplets or cavitation bubble collapse still remain as the topics of interest and require further investigation and research.

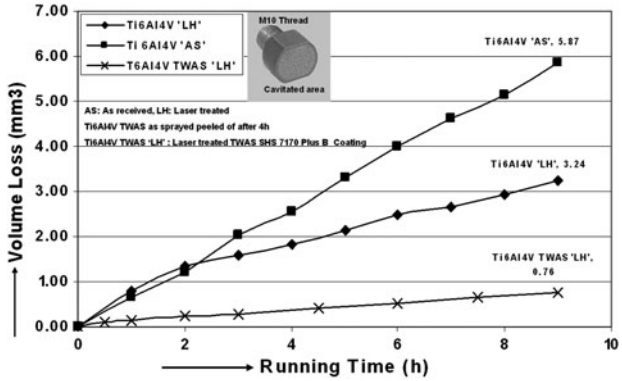

Fig. 1 Volume loss of laser-treated TWAS SHS 7170$^{Plus\ B}$ coating along with other materials up to 9 h of CE testing as per ASTM-G 32-2003

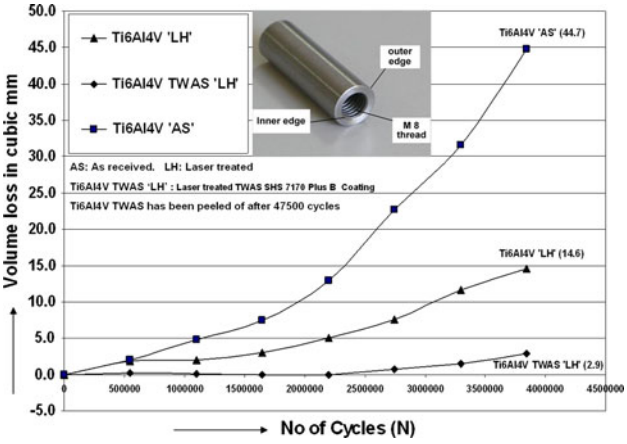

Fig. 2 Volume loss of laser-treated TWAS SHS 7170$^{Plus\ B}$ coating along with other materials up to 3.84 million cycles in WDE as per ASTM-G-73-1998 at an energy flux of 57.167 million J/m^2·s

3.2 Surface Damage

The scanning electron micrographs (SEM) of WDE- and CE-eroded HPDL-treated TWAS-coated samples are shown in Fig. 4(a, b) and Fig. 5(a, b), respectively. From the micrographs, it is observed that micro cavities are being formed on the surfaces for both WDE- and CE-eroded samples, and these occur more in the case of cavitation. Some information on the SEM of both cavitation- and water impingement-eroded 18-8 stainless steel samples is available in Ref 27. It has been reported that the plastic deformation occurred inside the crystal grain, whereas cracks and deep grooves appeared on the grain boundary because of the high impact of cavitation bubble collapse, resulting in material removal. It has been concluded that the cavitation and water-impingement erosion damages that occur on this material are similar. In the present investigation, material removal appears to be different to that reported in Ref 27. This may be because the HPDL-treated TWAS coating is hard and brittle. For both WDE- and CE-eroded samples, cleavage-type damage and material removal grain by grain are observed.

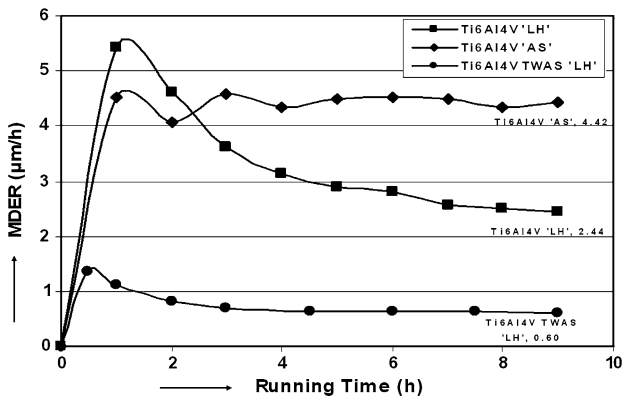

Fig. 3 MDER of laser-treated TWAS SHS 7170$^{Plus\ B}$ coating along with other materials up to 9 h of CE testing as per ASTM-G 32-2003

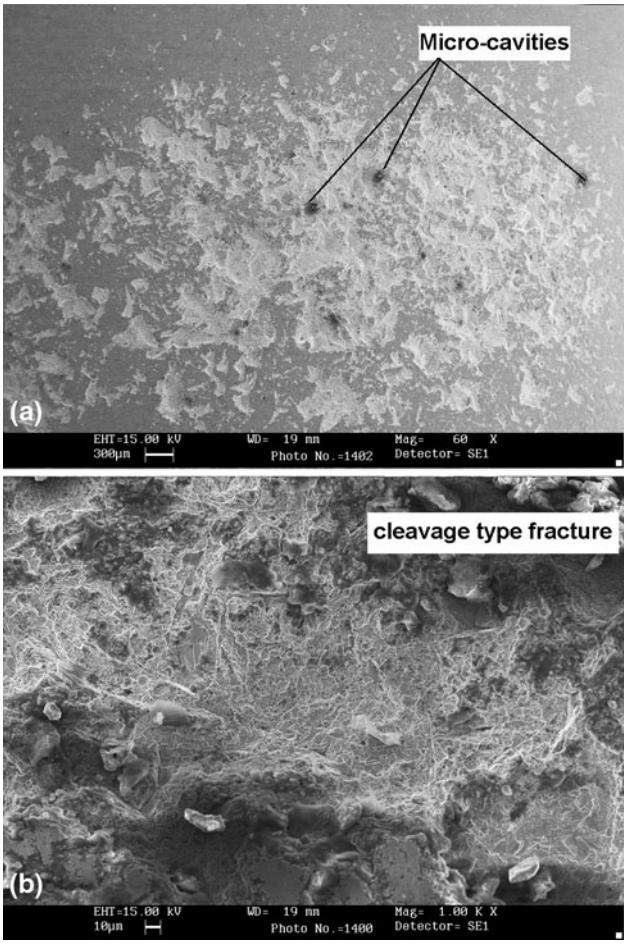

Fig. 4 (a) Showing SEM of laser-treated TWAS SHS 7170$^{Plus\ B}$ coating after WDE testing of 3.84 million cycles (micro-cavities visible); and (b) showing SEM of laser-treated TWAS SHS 7170$^{Plus\ B}$ coating after WDE testing of 3.84 million cycles (cleavage type damage visible)

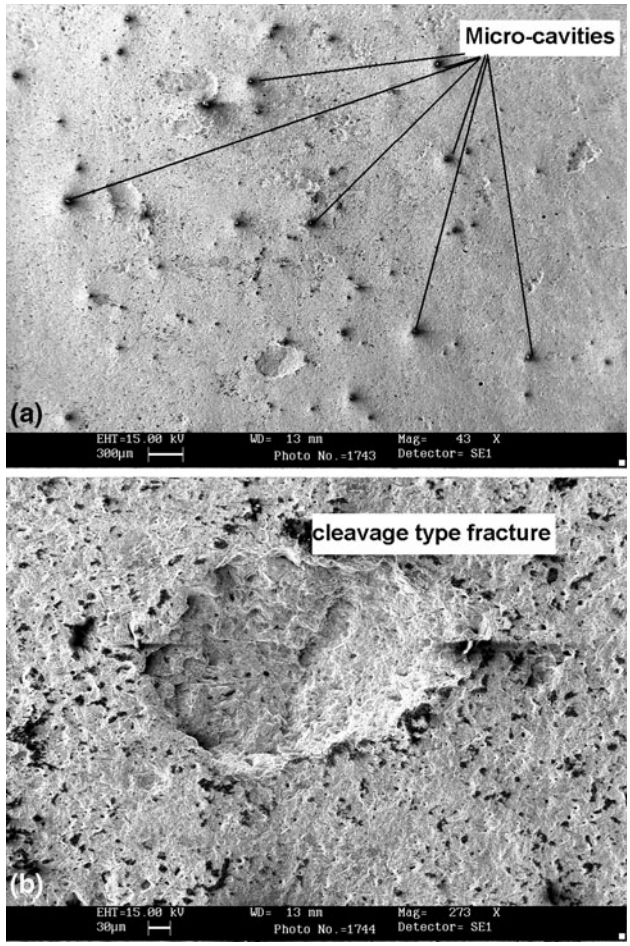

Fig. 5 (a) Showing SEM of laser-treated TWAS SHS 7170$^{Plus\ B}$ coating after CE testing of 5 h (micro-cavities visible); and (b) showing SEM of laser-treated TWAS SHS 7170$^{Plus\ B}$ coating after CE testing of 5 h (cleavage-type damage visible)

4. Conclusions

The laser-treated TWAS SHS 7170$^{Plus\ B}$-coated Ti6Al4V alloy sample has better adhesion and toughness as compared to the untreated one and, hence, gives much better performance in cavitation and WDE testings. The "as sprayed" TWAS SHS 7170 coating has peeled off during initial cavitation and WDE testings because it has voids, pores, and inter-boundary defects which are the inherent defects in these coatings.

From the SEM of the laser-treated TWAS SHS 7170$^{Plus\ B}$-coated sample, it is observed that micro cavities are being formed on the surfaces for both WDE- and CE-eroded samples, and these occur more in the case of cavitation. Material removal methods for both the above erosion mechanisms are similar. The volume loss trends of WDE and CE for Ti6Al4V alloy (coated, uncoated, and laser treated) are also similar. The materials and coatings, which have performed extremely well in WDE, have also performed very well in the CE.

Cavitation erosion testing as per ASTM G-32-2009 or ASTM G134-95 (2006) can be used for grading materials and coatings in droplet erosion instead of the more expensive, time-consuming, and cumbersome WDE testing as per ASTM G-73-2010.

Acknowledgment

The authors are thankful to the management of BHEL Corporate R&D for their permission to publish this article.

References

1. W.F. Adler, Ed., *Erosion: Prevention and Useful Applications*, ASTM STP 664, Philadelphia, PA, 1979, 643 pp
2. M. Lesser, Thirty Years of Liquid Impact Research: A Tutorial Review, *Wear*, 1995, **186-187**, p 28–34
3. J.E. Field, J.P. Dear, and J.E. Ogren, The Effects of Target Compliance on Liquid Drop Impact, *J. Appl. Phys.*, 1989, **65**, p 540–553
4. M.B. Lesser and J.E. Field, The Impact of Compressible Liquids, *Annu. Rev. Fluid Mech.*, 1983, **15**, p 97–122
5. J.E. Field, ELSI, Conference: Invited Lecture Liquid Impact: Theory, Experiment, Applications, *Wear*, 1999, **233-235**, p 1–12
6. H.C. Man, Z.D. Cui, T.M. Yue, and F.T. Cheng, Cavitation Erosion Behavior of Laser Gas Nitrided Ti and Ti6Al4V Alloy, *Mater. Sci. Eng. A*, 2003, **355**, p 167–173
7. B.S. Mann, V. Arya, B.K. Pant, and M. Agarwal, High-Power Diode Laser Surface Treatment to Minimize Droplet Erosion of Low-Pressure Steam Turbine Moving Blades, *J. Mater. Eng. Perform.*, 2009, **18**(7), p 990–998
8. B.S. Mann, V. Arya, and B.K. Pant, Enhanced Erosion Protection of TWAS Coated Ti6Al4V Alloy Using Boride Bond Coat and

Subsequent Laser Treatment, *J. Mater. Eng. Perform.*, 2010. doi: 10.1007/s11665-010-9735-9

9. B.S. Mann, V. Arya, and B.K. Pant, Influence of Laser Power on the Hardening of Ti6Al4V Low Pressure Steam Turbine Blade Material for Enhancing the Water Droplet Erosion Resistance, *J. Mater. Eng. Perform*., 2011, **20**(2), p 213–218
10. L. Gerke, J. Stella, J.C. Schauer, M. Pohl, and J. Winter, Cavitation Erosion Resistance of a-C:H Coatings Produced by PECVD on Stainless Steel and NiTi Substrates, *Surf. Coat. Technol.*, 2010, **204**, p 3418–3424
11. C.P. Qin, Y.G. Zheng, and R. Wei, Cavitation Erosion Behavior of Nanocomposite Ti-Si-C-N and Ti/Ti-Si-C-N Coatings Deposited on 2Cr13 Stainless Steel Using a Plasma Enhanced Magnetron Sputtering Process, *Surf. Coat. Technol.*, 2010, **204**, p 3530–3538
12. B.K. Pant, V. Arya, and B.S. Mann, Enhanced Droplet Erosion Resistance of Laser Treated Nano Structured TWAS and Plasma Ion-Nitro Carburized Coatings for High Rating Steam Turbine Components, *J. Therm. Spray Technol.*, 2010, **19**(5), p 884–892
13. Y.I. Oka and H. Miyata, Erosion Behaviour of Ceramic Bulk and Coating Materials Caused by Water Droplet Impingement, *Wear*, 2009, **267**, p 1804–1810
14. M. Ahmad, M. Casey, and N. Surken, Experimental Assessment of Droplet Impact Erosion Resistance of Steam Turbine Blade Materials, *Wear*, 2009, **267**, p 1605–1618
15. Y.I. Oka, S. Mihara, and H. Miyata, Effective Parameters for Erosion Caused by Water Droplet Impingement and Applications to Surface Treatment Technology, *Wear*, 2007, **263**, p 386–394
16. F.T. Cheng, K.H. Lo, and H.C. Man, NiTi Cladding on Stainless Steel by TIG Surfacing Process Part I. Cavitation Erosion Behavior, *Surf. Coat. Technol.*, 2003, **172**, p 308–315
17. F.T. Cheng, K.H. Lo, and H.C. Man, NiTi Cladding on Stainless Steel by TIG Surfacing Process Part II. Corrosion Behavior, *Surf. Coat. Technol.*, 2003, **172**, p 316–321
18. K.H. Lo, F.T. Cheng, C. Kwok, and H.C. Man, Improvement of Cavitation Erosion Resistance of AISI, 316 Stainless Steel by Laser Surface Alloying Using Fine WC Power, *Surf. Coat. Technol.*, 2003, **165**, p 258–267
19. C.T. Kwok, F.T. Cheng, and H.C. Man, Laser-Fabricated Fe-Ni-Co-Cr-B Austenitic Alloy on Steels. Part I. Microstructures and Cavitation Erosion Behaviour, *Surf. Coat. Technol.*, 2001, **145**, p 194–205
20. C.T. Kwok, F.T. Cheng, and H.C. Man, Laser-Fabricated Fe-Ni-Co-Cr-B Austenitic Alloy on Steels. Part II. Corrosion Behaviour and Corrosion-Erosion, *Surf. Coat. Technol.*, 2001, **145**, p 206–214
21. R.J. Hand and J.E. Field, Liquid Impact on Toughened Glasses, *Eng. Fract. Mech.*, 1990, **37**(2), p 293–311
22. M. Duraiselvam, R. Galun, S. Siegmann, V. Wesling, and B.L. Mordik, Liquid Impact Erosion Characteristics of Martensitic Stainless Steel Laser Clad with Ni-Based Intermetallic Composites and Matrix Composites, *Wear*, 2006, **261**, p 1140–1149
23. J. Steller, International Cavitation Erosion Test and Quantitative Assessment of Material Resistance to Cavitation, *Wear*, 1999, **233-235**, p 51–64
24. W.F. Adler, The Mechanisms of Liquid Impact, *Erosion*, C.M. Preece, Ed., Academic Press, New York, 1979, p 127–184
25. J.H. Brunton and M.C. Rochester, Erosion of Solid Surfaces by the Impact of Liquid Drops, *Erosion*, C.M. Preece, Ed., Academic Press, New York, 1979, p 185–248
26. F.J. Heymann, On Shock Wave Velocity and Impact Pressure in High Speed Liquid-Solid Impact, *Trans. ASME J. Basic Eng.*, 1968, **90**, p 400–402
27. S. Hattori and M. Takinami, Comparison of Cavitation Erosion Rate with Liquid Impingement Erosion Rate, *Wear*, 2010, **269**, p 310–316
28. A. Krella, The Experimental Resistance Parameter for TiN Coating to Cavitation Action, *Adv. Mater. Sci.*, 2010, **10**(1), p 4–18
29. A. Krella, Cavitation Resistance of TiN Nanocrystalline Coatings with Various Thickness, *Adv. Mater. Sci.*, 2009, **9**(2), p 12–24
30. R. Hiking, Transient, High-Pressure Solidification Associated with Cavitation in Water, *Phys. Rev. Lett.*, 1994, **73**, p 2853–2856